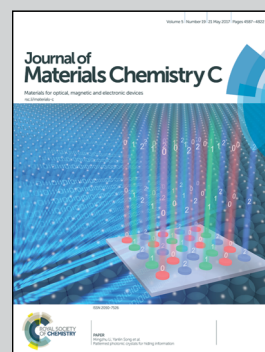**Showcasing research from the School of Materials Science and Engineering, Wuhan University of Technology, China.**

Colloidal stable quantum dots modified by dual functional group polymers for inkjet printing

Novel water-dispersible QDs inks capped with hyperbranched mercaptopropionic polyethylenimine (MPPEI) exhibit strong fluorescence and excellent colloidal stability, and are very promising for inkjet printing for security documents.

ROYAL SOCIETY
OF CHEMISTRY

rsc.li/materials-c

ROYAL SOCIETY OF CHEMISTRY

PAPER

Check for updates

Colloidal stable quantum dots modified by dual functional group polymers for inkjet printing†

Ting Han, [ID] Ye Yuan, Xiao Liang, Yang Zhang, Chuanxi Xiong and Lijie Dong*

Quantum dots (QDs) with unique fluorescence properties have been applied in a variety of applications. Here, we report an effective method to prepare water-dispersible QDs that have remarkable colloidal stability and can be used in inkjet printing. A new dual functional group polymer, mercaptopropionic polyethylenimine (MPPEI), as a ligand combines the thiol of 3-mercaptopropionic acid (MPA) with the amine of polyethylenimine (PEI) for the surface functionalization of CdSe/CdS/ZnS quantum dots (QDs). These ligands reduce issues of thiol oxidation and the weak binding affinity of the amino group. Ligation with these polymers provides fluorescent QDs with excellent acid resistance, base resistance, photostability and thermostability, since the branched structure of MPPEI can provide QDs with very effective protection. We use these stable QDs as security inks and obtain a fluorescent pattern that is invisible under ambient light.

Introduction

Highly luminescent quantum dots (QDs) have attracted widespread attention in the past two decades due to their unique electrical and optical properties, which depend on the size, shape and surface chemistry of the QDs and can be adjusted through surface modification.[1,2] These optical and chemical characteristics have generated great interest in developing QDs for use in light emitting diodes, solution-processed solar cells and bimolecular imaging.[3–8]

Recently, QDs have been actively studied as functional inks, since anti-counterfeiting technology in printing has been of great interest.[9–24] Sun *et al.* achieved fluorescent patterns by using an ink prepared by incorporating La-doped ZnO QDs into a transparent oil.[25] Small *et al.* used water-dispersible Mn^{2+}-doped ZnS quantum dots as inkjet printing inks and obtained fluorescent images printed onto photographic-quality inkjet paper.[26] Furthermore, ZnS QDs, CdTe QDs, CdSe/ZnS core/shell QDs and so on have been used to print luminescent images successfully.[27–32] From a security perspective, QD-based inks have a great advantage due to their bright fluorescence under UV light. Water-dispersible QD inks have lower viscosity and better fluidity, and are easily absorbed by the printing paper.[26] In addition, the volatile water will cause far less pollution to the environment than volatile organic solvents. All of these advantages make water-dispersible QDs excellent candidates for security documents, encryption and labels.

Challenges remain, however, as QDs with narrow size distributions and the desired optical properties are commonly synthesized in organic solvents.[33–36] As a result, these QDs obtain extremely hydrophobic ligands from the surfactants used in the synthesis (mostly trioctylphosphine oxide (TOPO) and/or trioctylphosphine (TOP)), which makes it difficult for the QDs to be dispersed in water.[37] Hence, the hydrophilization of the surface of the QDs is an essential prerequisite for water dispersible and highly stable QDs.

Currently, ligand exchange is simple and effective, and is the most popular successful strategy for surface modification.[38] Thiol ligands have been extensively studied and are among the most prevalent ligands used for ligand exchange because of their strong coordination to QDs, the simple exchange process and the resulting exposed carboxyl groups, which provide water solubility and further functionalization for QDs.[39] However, the binding of thiol ligands on the surface of QDs strongly influences the electron and hole wavefunctions.[40] It was reported that the use of thioalkyl acid ligands results in a substantial decrease in the QY compared to the standard TOP/TOPO ligands.[41] In addition, thiol molecules are easily oxidized and thus quench the band edge photoluminescence (PL) in QDs by extracting holes from the surface.[42] As a result, these QDs cannot survive for a long time, and the fluorescence of these QDs is quickly quenched under strongly acidic conditions.[43]

In addition to thiol ligands, dendrimers with amino groups are effective multidentate ligands that have a high density of functional groups. Hyperbranched PEI as a topical dendrimer that contains substantial amounts of amino groups and aliphatic chains can endow QDs with amphiphilic performance.[44,45] Moreover, the higher water solubility of PEI can effectively

School of Materials Science and Engineering, Wuhan University of Technology, Luoshi Road 122, Wuhan, 430070, P. R. China. E-mail: dong@whut.edu.cn

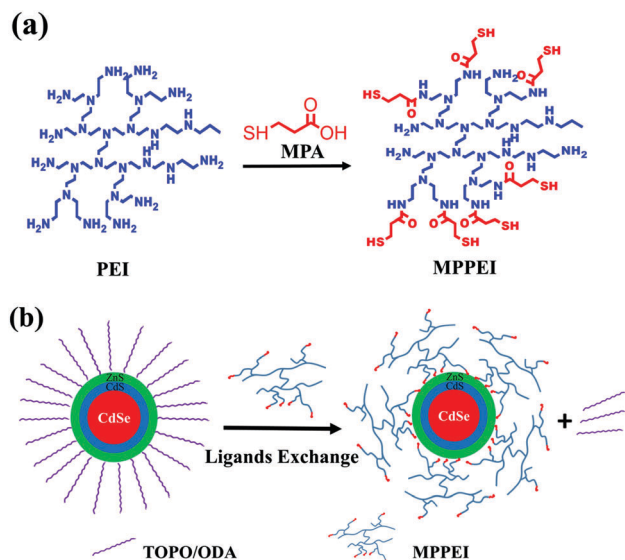† Electronic supplementary information (ESI) available. See DOI: 10.1039/c7tc00452d

This journal is © The Royal Society of Chemistry 2017

J. Mater. Chem. C, 2017, 5, 4629–4635 | 4629

Fig. 1 The synthetic route for preparing (a) the thiol- and amine-based ligand MPPEI, and (b) MPPEI-capped QDs.

transform hydrophobic QDs into water-dispersible QDs. However, it has been reported that QDs transformed using PEI are more likely to be unstable.[46] It is assumed that both the high steric hindrance of PEI and the relatively weaker coordination of amino groups to the semiconductor result in the low stability of QDs/PEI.

Herein, we report a new kind of ligand, mercaptopropionic polyethylenimine (MPPEI), synthesized by reaction of MPA with PEI, and use it as a stable surface coating to stabilize the fluorescence of QDs. Fig. 1(a) shows a schematic representation of the general synthetic route used to prepare this thiol- and amine-based ligand. The reaction equation is shown in Fig. S1 (ESI†). The as-prepared QDs exhibit good stability in a wide pH range, under UV light and at high temperature due to the core/shell/shell structure of the QDs and the branched structure of MPPEI. Compared to core/shell QDs, the CdSe/CdS/ZnS QDs have much greater stability due to the protection provided by the outer ZnS layer, which provides efficient confinement of electron and hole wave functions inside the nanocrystal shell, and the middle CdS shell, which allows a considerable reduction in the strain inside the nanocrystals.[47–49] The large number of acid and base groups and the branched structure of MPPEI enable it to have strong coordination on the QDs and buffer pH changes by rapidly absorbing or releasing protons.[50] We introduced these QDs for inkjet printing. As expected, a clear image with strong luminescence was printed using the QDs/MPPEI inks. The water dispersibility, strong fluorescence and high colloidal stability of the inks and the high quality of the printed images all demonstrate that QDs/MPPEI could be an ideal invisible security ink for information coding.

Experimental section

Materials

Cadmium oxide (CdO, 99.99%), zinc oxide (ZnO, 99.99%, powder), selenium (Se, 99.5%), sulfur (S, 99.98%, powder),

tributylphosphine oxide (TOPO, 90%), tributylphosphine (TBP, 97%), octadecylamine (ODA, 97%), 1-octadecene (ODE, 90%), oleic acid (OA, 90%), stearic acid (SA, 99%), 3-mercaptopropionic acid (MPA, 98%), and hyperbranched polyethylenimine (PEI) were all purchased from Sigma-Aldrich. *N,N*-Dicyclohexylcarbodiimide (DCC, CP), *N*-hydroxysuccinimide (NHS, BR), sodium hydroxide (NaOH, AR), hydrochloric acid (HCl, AR), hexane, trichloromethane, acetone, and *N,N*-dimethylformamide (DMF) were purchased from Sinopharm Chemical Reagent Co. Ltd, and normal non-fluorescent printing paper was purchased from Laiyang JETCO Paper Co. Ltd.

Synthesis of CdSe/CdS/ZnS core/shell/shell QDs

The CdSe/CdS/ZnS QDs used in this study were prepared according to a version of a previously reported method.[51] Firstly, ODA-capped CdSe nanocrystals were initially synthesized by injecting a pre-calculated amount of TBP-Se precursor into Cd-SA stock solutions at high temperature after vacuum pumping and purging with nitrogen gas many times. Then, the successive ion layer adsorption and reaction (SILAR) technique allows complex shells to be grown around a given CdSe-core particle.[52] The further layers of CdS based on the CdSe QDs include one monolayer of $Cd_{0.5}Zn_{0.5}S$ and another layer of ZnS. For each shell growth, a calculated amount of the appropriate precursor solution was injected with a syringe using standard air-free procedures. The as-synthesized CdSe/CdS/ZnS core/shell/shell QDs were stored in the dark as a stock solution. The as-synthesized QDs with red fluorescence exhibit a high PL quantum yield (QY) as high as 70% at room temperature.

Ligand design

A suitable amount of MPA was added dropwise into a solution containing DCC and NHS dissolved in DMF. Subsequently, excess PEI was added into the DMF solution. The reaction was then carried out with magnetic stirring for 24 h. Then the reaction mixture was precipitated in acetone. After centrifugation, the supernatant containing excess DCC, NHS and DMF was discarded and the precipitate was a viscous amber gel. The DMF was removed by placing the precipitate under vacuum and drying at 120 °C for 24 h. The precipitate was then redispersed in water.

Preparation of water-dispersible QDs

QDs/MPPEI were prepared by ligand exchange as shown in Fig. 1(b). The as-synthesized QDs were dispersed in hexane. Addition of three times the volume of acetone to the aliquot results in the reversible flocculation of the QDs. The flocculate is separated from the supernatant by centrifugation, then flocculated in chloroform. An excess of MPPEI water solution was added to the hydrophobic QDs in chloroform. The mixture was subjected to ultrasonic treatment at room temperature in the absence of light for 3 hours. The QD samples were precipitated by adding excess acetone and centrifuged at 5000 rpm for 10 min yielding a red pellet. The clear supernatant was discarded and the pellet was redissolved in chloroform, followed by another round of precipitation using excess acetone. The precipitate was dried under vacuum, then dispersed in distilled water. Bath sonication was applied for 90 minutes to promote the dispersion of the

nanoparticles. The QD dispersion was subsequently cleaned by dialysis for 4 days in a dialysis tube (MD34 (8000–14 000)) against deionized water to remove the excess ligands. The QDs/MPPEI dispersion was diluted to a concentration of 0.5 mg ml^{-1} by adding distilled water. The pH of the system was adjusted to be 7.0 by using 10 mM HCl and measured using a digital pH meter.

Quantum yield (QY) measurements

The QY values of the original CdSe/CdS/ZnS QDs and the QDs/MPPEI were calculated using a reference method.[53] An ethanol solution of rhodamine 6G was used as a standard, which has a QY of 95%. The following equation was then used:

$$\phi_{QD} = \phi_{Std}\left(\frac{A_{Std}}{A_{QD}}\right)\left(\frac{I_{QD}}{I_{Std}}\right)\left(\frac{n_{QD}}{n_{Std}}\right)^2$$

where φ is the QY, A is the absorption value under 480 nm excitation, I is the fluorescence integral intensity and n is the refractive index at room temperature. The subscripts "Std" and "QD" refer to the standard rhodamine solution and QDs, respectively.

Inkjet printing

A 0.5 mg ml^{-1} QDs/MPPEI dispersion with a pH of 7.0 was inserted into an ink cartridge and ink-jet printed by an Epson L 130 inkjet printer at room temperature. Commercially available printing paper with no background UV fluorescence on which the QDs adhered well was chosen as the printing paper. The logo of Wuhan University of Technology as a complex circle pattern was printed and dried at room temperature. We observed the images under 365 nm UV light using a hand-held UV lamp and took photographs of the pattern using a Sony a5000 digital camera.

Characterization

TEM (Joel JEM-2001F) images of the QDs were obtained at an acceleration voltage of 200 kV. Carbon-supported copper grids were dipped in a diluted dispersion with an absorbance of the first absorption peak of the nanocrystals below 0.2 and then dried prior to observation. IR measurements were made on an FTIR spectrometer (Thermo Nicolet Nexus) using KBr pellets. The zeta potential of the QDs was measured using a Malvern Zetasizer Nano ZS90, which converted the electrophoretic mobility to a zeta potential using Smoluchowski approximation. The error bars represent the standard deviation. The pH values of the QDs/MPPEI dispersions were adjusted using 0.2 M HCl and 0.2 M NaOH with a digital pH meter (PHS-3C, LEICI). UV-vis absorption spectra and PL emission spectra were measured on a RF-5301 PC fluorometer. The PL quantum yields of a diode array UV-vis spectrometer (UV-2550, SHIMADZU) and the samples were estimated by comparing the integrated fluorescence intensity to that of rhodamine 6G with a known quantum yield (95% in ethanol) as the standard. Both the QD samples and the standard solution were excited at 480 nm.

Results and discussion

Morphology and structure analysis

In order to examine the microstructure and dispersion of the QDs, transmission electron microscopy (TEM) analysis of the pristine QDs in hexane and the resulting QDs/MPPEI in water was carried out. The CdSe/CdS/ZnS core/shell/shell QDs synthesized by pyrolysis in an oil phase appeared spherical and fairly monodisperse without any aggregation, as shown in Fig. 2(a) and (b). As can be clearly seen in the insets of Fig. 2(a) and Fig. S3(a) (ESI†), the QDs, with an average diameter of 4.92 nm, are red under both daylight and UV light. Owing to the strong coordination between –SH and metal ions, the as-prepared MPPEI was designed to decorate the QDs *via* ligand exchange. The great number of free hydrophilic amino groups of dendritic PEI provide the QDs with excellent dispersity in water. As a result, the QDs/MPPEI, with an average diameter of about 5 nm, exhibit perfect monodispersity as shown in Fig. 2(c) and Fig. S2, S3(b), S3(c) (ESI†). In addition, the water-dispersible CdSe/CdS/ZnS QDs can be easily detected under UV light, while they are almost transparent in daylight. The high-resolution images in the insets of Fig. 2(b) and (d) show lattice fringes, indicating that the as-prepared QDs are highly crystallized, and the clear lattice fringes indicate that ligand exchange did not change the crystal structure of the QDs.

The corresponding energy-dispersive X-ray (EDX) spectrum demonstrated the presence of Cd, Se, S, Zn and O elements in the QDs/MPPEI sample, as shown in Fig. 3(a). The N peak at
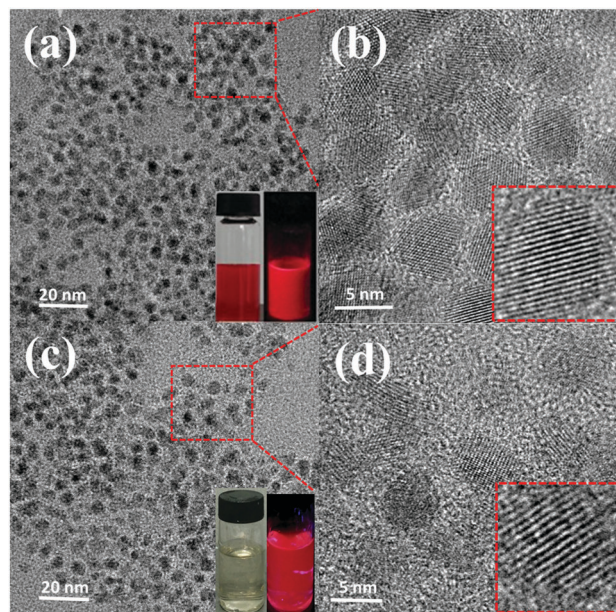

Fig. 2 (a) TEM image of CdSe/CdS/ZnS QDs with a scale bar of 20 nm; the inset is QDs dispersed in *n*-hexane under daylight and 365 nm UV light. (b) TEM image of CdSe/CdS/ZnS QDs with a scale bar of 5 nm; the inset is a high-resolution image. (c) TEM images of QDs/MPPEI with a scale bar of 20 nm; the inset is QDs/MPPEI dispersed in water under daylight and 365 nm UV light. (d) TEM images of QDs/MPPEI with a scale bar of 5 nm; the inset is a high-resolution image. The concentration of the QDs/MPPEI dispersion in (c) and (d) is 0.05 mg ml^{-1}.
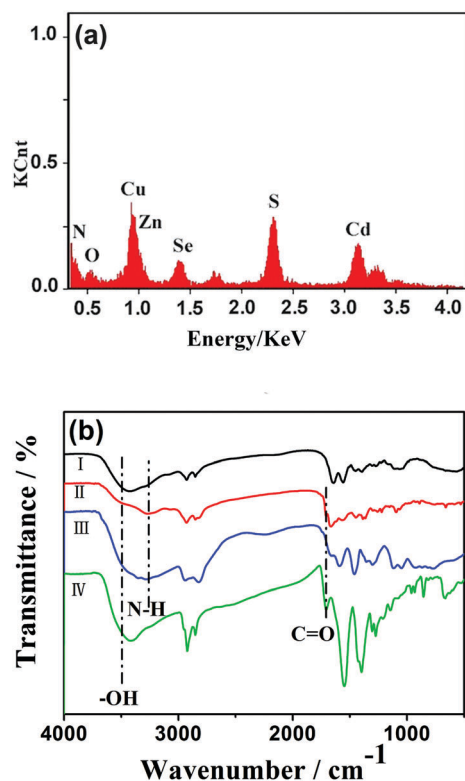
Fig. 3 (a) EDX spectrum of QDs/MPPEI, and (b) FT-IR spectra of (I) QDs/MPPEI, (II) MPPEI, (III) PEI and (IV) MPA.

Fig. 4 Zeta potential *versus* pH of the QDs/MPPEI.

0.3924 keV could indicate that the MPPEI ligands have replaced the original TOPO/ODA ligands on the surface of the QDs. In general, high amounts of N element are required to detect the characteristic N signal peak due to the interference of the C and O element peaks.

The surface groups of QDs/MPPEI, MPPEI, PEI and MPA were investigated by FTIR spectroscopy, as shown in Fig. 3(b). Comparing (II), (III) and (IV), the gross resemblance of both the spectral features and peak positions for several vibrational modes, such as N–H stretching (3336 cm^{-1}), C–H stretching (2800–3000 cm^{-1}) and bending (1340 cm^{-1}), and especially the C=O stretching motion of the ester functional group at 1732 cm^{-1}, guarantees the successful combination of MPA onto the PEI chain. The FTIR spectra of these functional groups (–SH and –NH_2) on the QDs in Fig. 3(b) (I) combined with the EDX results indicated that the QDs were successfully capped by MPPEI.

The zeta potentials of the QDs/MPPEI are shown in Fig. 4. The isoelectric point (IEP) was determined to be at pH = 8.9. When the pH value was lower than 7, there was a significant decrease in the positive charge with an increase in the pH value. The stability of the QDs in an aqueous dispersion is attributed to the positive charge of the particles generated by the protonation of the –NH_2 groups with the formation of –NH_3^+. With increasing pH value, the nanoparticles gain a rich negative charge due to –SH groups and remain stable.[54] The like-charges on the nanoparticles reduce the repulsive electrostatic forces between the nanoparticles, resulting in less agglomeration and the high stability of the QDs.
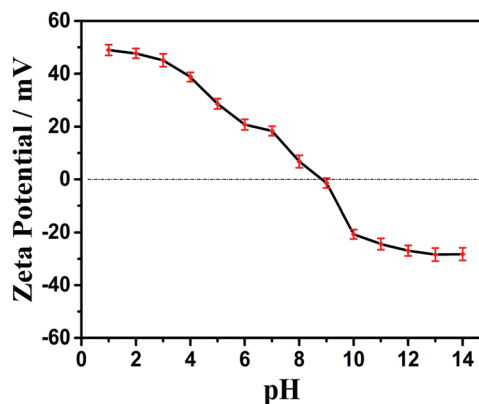
Optical property analysis

The optical properties of the QDs capped with the original TOPO/ODA ligands and capped with MPPEI in water have been investigated by UV-vis spectrometry and PL spectroscopy. Fig. 5a shows the similar absorption behaviours of the QDs and QDs/MPPEI, which indicates that the internal structure of the QDs was not destroyed during ligand exchange. Compared with the original QDs, the peak shape and half-peak width is almost unchanged, as shown in Fig. 5(b). The original hydrophobic QDs showed strong fluorescence, with symmetrical emission at 630 nm. The quantum yield of the original CdSe/CdS/ZnS QDs was measured to be as high as 70%. Following phase transfer to water, the PL QY of the QDs/MPPEI changed to be about 50%, which is consistent with recent reports.[55–57] The decrease in the quantum yield is attributed to the increase in the number of dangling bonds during ligand exchange.

Colloidal stability tests

Although QDs possess strong fluorescence, their colloidal stability under different conditions is still a notable problem. To illustrate the stability of the QDs/MPPEI, their luminescence and absorbance in different pH environments was investigated. It is clear that the PL intensity of the QDs/MPPEI remained constant at extremely low pH, and the absorbance was unchanged at pH = 1 after 100 min, as shown in Fig. 6(a) and Fig. S4(a) (ESI†). This can be explained by the positive charges on the nanoparticles inducing repulsive electrostatic forces. The three-dimensional
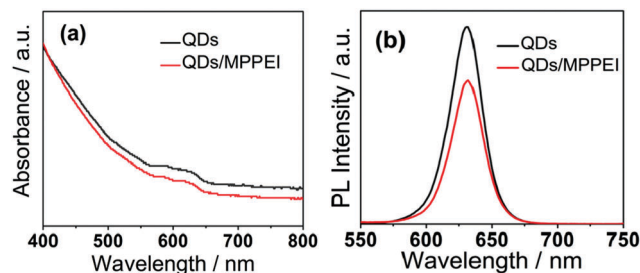

Fig. 5 UV-vis spectra of the QDs and QDs/MPPEI (a), and PL spectra of the QDs and QDs/MPPEI (b).
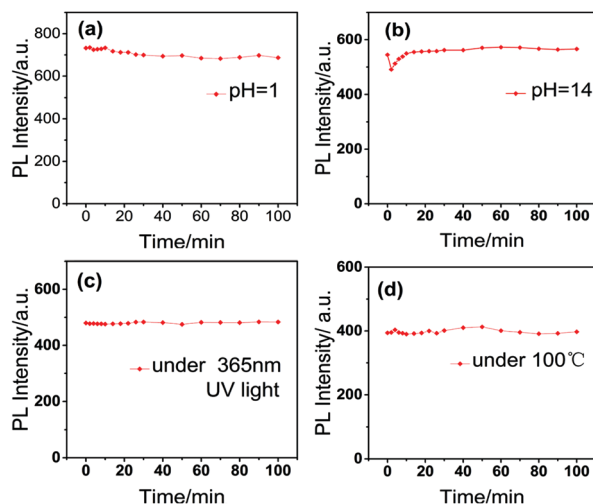
Fig. 6 PL intensity of QDs/MPPEI before and after treatment with (a) strong acid, (b) strong base, (c) UV light and (d) high temperature.
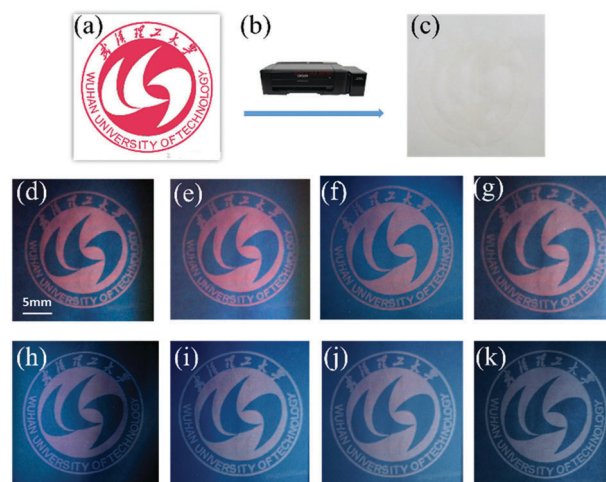

Fig. 7 The original image (a), the inkjet printer (b), and images of the non-fluorescent ink-jet paper with the logo printed with QDs/MPPEI solution viewed under ambient light (c), and viewed under 365 light (d), after 10 days (e), 20 days (f), 30 days (g), 40 days (h), 50 days (i), 60 days (j) and 70 days (k).

structure of PEI provides effective protection for the QDs.[58] In contrast to what was observed for the QDs in acid, a decrease in fluorescence intensity was observed at pH 14 after about 5 min, as shown in Fig. 6b, likely due to the instability of the QD core in basic solutions, and then gradually increased soon afterwards. This effect may be attributed to both the repulsive electrostatic forces and the formation of a $Zn(OH)_2$ passivation shell on the surface of the QDs, which effectively eliminates the non-radiative recombination of charge carriers.[59] Therefore the UV-vis spectra of the QDs/MPPEI after 100 min of base treatment were unchanged, as shown in Fig. S4(b) (ESI†). This pH stability test proved that the water-dispersible QDs possess excellent fluorescence stability under extreme pH conditions and can be applied in a large pH range.

Generally, illumination and temperature are also as important as pH for QD stability. So, for further investigation, photo-stability and thermal stability tests were carried out. Fig. 6(c) shows the dependence of the fluorescence intensity on the time of UV irradiation. The QDs/MPPEI fluorescence intensity and absorbance was almost unchanged throughout the test time (100 min) under UV illumination at pH = 7.0, as shown in Fig. 6(c) and Fig. S4(c) (ESI†), which indicates that the water-dispersible QDs exhibit stable fluorescence under continuous UV light. The photostability of the QDs was due to protection from the shells of the QDs and the outermost MPPEI. Fig. 6(d) and Fig. S4(d) (ESI†) show the PL intensity and UV spectra of the QDs at 100 °C. There are no significant changes either in the PL intensity or the absorbance, which illustrates the favourable thermal stability of the QDs. Therefore, it can be concluded from these results that these QDs possess excellent colloidal stability at extreme pH, under UV light and at high temperature.

Inkjet printing of patterns using the water dispersible QDs as ink

From what has been discussed above, we have demonstrated that the water dispersible QDs/MPPEI synthesized by ligand exchange possess strong fluorescence under 365 nm UV light

and remarkable colloidal stability in different environments. Their excellent optical performance enabled the QDs to be readily employed as a fluorescent ink with a solvent of water and at a lower concentration of 0.5 mg ml^{-1} compared to many other nanoparticle inks, making them more environmentally friendly and economical.[25–32] A kind of common commercial non-fluorescent paper was employed as the printing paper in order to reduce the interference of background UV fluorescence. Images of the complex pattern shown in Fig. 7(a) were printed with the QDs/MPPEI ink. As the QDs/MPPEI aqueous dispersion was almost transparent, there was a blurred, nearly invisible pattern on the paper under ambient light (Fig. 7(c)), which is of great significance for security. Unsurprisingly, a red image was clearly visible when the paper was viewed under 365 nm UV light, as shown in Fig. 7(d). The paper with the as-printed pattern was kept at room temperature. Photos of the printed pattern under UV light were then taken every 10 days. As we can see, the red color is nearly unchanged after 30 days, as shown in Fig. 7(g), mainly due to the remarkable protection of the QDs by the MPPEI ligands. As time went on, although the color faded a little, it was noted that the pattern was still clearly visible and the brightness changed little. After 70 days, the image was still clear under UV light, although there was some slight discoloration, as shown in Fig. 7(k). Based on these characteristics, the QD-based inks are much more suitable for image printing. The above results combined are promising and further confirm that the as-prepared hydrophilic QDs could be used as functional inks for inkjet printing.

Conclusions

We present an effective approach to synthesize water-dispersible QDs. A versatile nanoparticle construct using an MPA and PEI coating on a highly robust CdSe/CdS/ZnS core/shell/shell structure

This journal is © The Royal Society of Chemistry 2017

J. Mater. Chem. C, 2017, 5, 4629–4635 | 4633

to form aqueous QDs showed high stability and good fluorescence properties. As the outermost part of the QDs/MPPEI, the hyperbranched PEI has a protective effect on the MPA, thus reducing thiol oxidation and improving the fluorescence stabilities of the luminescent QDs.

These stable water-dispersible QDs were successfully applied as inkjet printing inks for information storage and could only be read under UV light. Moreover, the printed image could retain a clear pattern after at least 70 days. We suggest that these new functional inks could be efficient in inkjet printing and have potential use in document security.

Acknowledgements

Notes and references

1 A. P. Alivisatos, *Science*, 1996, **271**, 933.

2 A. L. Efros and M. Rosen, *Annu. Rev. Mater. Sci.*, 2000, **30**, 475.

3 X. L. Dai, Z. X. Zhang, Y. Z. Jin, Y. Niu, H. J. Cao, X. Y. Liang, L. W. Chen, J. P. Wang and X. G. Peng, *Nature*, 2014, **515**, 96.

4 A. H. Mueller, M. A. Petruska, M. Achermann, D. J. Werder, E. A. Akhadov, D. D. Koleske, M. A. Hoffbauer and V. I. Klimov, *Nano Lett.*, 2005, **5**, 1039.

5 J. W. Stouwdam and R. A. J. Janssen, *J. Mater. Chem.*, 2008, **18**, 1889.

6 A. P. Kumar, B. T. Huy, B. P. Kumar, J. H. Kim, V. D. Dao, H. S. Choi and Y. Lee, *J. Mater. Chem.*, 2015, **3**, 1957.

7 M. Graetzel, R. A. J. Janssen, D. B. Mitzi and E. H. Sargent, *Nature*, 2012, **488**, 304.

8 J. Zhang, G. Y. Hao, C. F. Yao, S. Hu, C. H. Hu and B. B. Zhang, *J. Mater. Chem. B*, 2016, **4**, 4110.

9 B. Duong, H. Liu, C. Li, W. Deng, L. Ma and M. Su, *ACS Appl. Mater. Interfaces*, 2014, **6**, 8909.

10 S. Olivier, L. Derue, B. Geffroy, T. Maindron and E. Ishow, *J. Mater. Chem. C*, 2015, **3**, 8403.

11 P. Kumar, J. Dwivedi and B. K. Gupta, *J. Mater. Chem.*, 2014, **2**, 10468.

12 N. Parvin and T. K. Mandal, *RSC Adv.*, 2016, **6**, 18134.

13 J. M. Meruga, W. Cross, M. Stanley, S. May and J. Kellar, *Nanotechnology*, 2012, **23**, 395201.

14 X. H. Chen, X. Y. Jin, J. J. Tan and H. T. Yang, *J. Colloid Interface Sci.*, 2016, **468**, 300.

15 V. Wood, M. J. Panzer, J. L. Chen, M. S. Bradley, J. E. Halpert, M. G. Bawendi and V. Bulovic, *Adv. Mater.*, 2009, **21**, 2151.

16 M. You, J. Zhong, Y. Hong, Z. Duan, M. Lin and F. Xu, *Nanoscale*, 2015, **7**, 4423.

17 E. Binetti, C. Ingross, M. Striccoli, P. Cosma, A. Agostiano, K. Pataky, J. Brugger and M. Curri, *Nanotechnology*, 2012, **23**, 075701.

18 C. Campos-Cuerva, M. Zieba, V. Sebastian, G. Martínez, J. Sese, S. Irusta, V. Contamina, M. Arruebo and J. Santamaria, *Nanotechnology*, 2016, **27**, 095702.

19 M. Böberl, M. V. Kovalenko, S. Gamerith, E. J. W. List and W. Heiss, *Adv. Mater.*, 2007, **19**, 3574.

20 A. Tang, Y. Liu, Q. Wang, R. Chen, W. Liu, Z. Fang and L. Wang, *Carbohydr. Polym.*, 2016, **148**, 29.

21 H. Zeng, D. Katagiri, T. Ogino, H. Nakajima, S. Kato and K. Uchiyama, *Anal. Chem.*, 2016, **88**, 6135.

22 S. Jeon, S. Park, J. Nam, Y. Kang and J. Kim, *ACS Appl. Mater. Interfaces*, 2016, **8**, 1813.

23 E. Petryayeva and W. R. Algar, *Anal. Bioanal. Chem.*, 2016, **408**, 2913.

24 B. Wang, A. Song, L. Feng, H. Ruan, H. Li, S. Dong and J. Hao, *ACS Appl. Mater. Interfaces*, 2015, **7**, 6919.

25 L. W. Sun, H. Q. Shi, W. N. Li, H. M. Xiao, S. Y. Fu, X. Z. Cao and Z. X. Li, *J. Mater. Chem.*, 2012, **22**, 8221.

26 A. C. Small, J. H. Johnston and N. Clark, *Eur. J. Inorg. Chem.*, 2010, 242.

27 B. H. Kim, M. S. Onses, J. B. Lim, S. Nam, N. Oh, H. J. Kim, K. J. Yu, J. W. Lee, J.-H. Kim, S.-K. Kang, C. H. Lee, J. Y. Lee, J. H. Shin, N. H. Kim, C. Lealand, M. Shim and J. A. Rogers, *Nano Lett.*, 2015, **15**, 969–973.

28 B. Bao, M. Li, Y. Li, J. Jiang, Z. Gu, X. Zhang, L. Jiang and Y. Song, *Small*, 2015, **11**, 1649.

29 H. Choi, T. Zhou, M. Singh and G. E. Jabbour, *Nanoscale*, 2015, **7**, 3338.

30 J. H. Johnston, A. C. Small and N. Clark, *Colour Tuneable Photoluminescent Quantum Dots for Ink-jet Printing of Security Documents and Labels*, Appita Inc, 2009.

31 S. Halivni, S. Shemesh, N. Waiskopf, Y. Vinetsky, S. Magdassi and U. Banin, *Nanoscale*, 2015, **7**, 19193.

32 P. Kumar, S. Singh and B. K. Gupta, *Nanoscale*, 2016, **8**, 14297.

33 W. Zou, Y. Ji, X. Wang, Q. Zhao, J. Zhang, Q. Shao, J. Liu, F. Wang and Y. Wang, *Chem. Eng. J.*, 2016, **294**, 323.

34 F. Wang, Z. Xie, B. Zhang, Y. Liu, W. Yang and C. Liu, *Nanoscale*, 2014, **6**, 3818.

35 M. Vaseem, R. Hong, R. Kim and Y. Hahn, *J. Mater. Chem. C*, 2013, **1**, 2112.

36 T. Lehnen, D. Zopes and S. Mathur, *J. Mater. Chem.*, 2012, **22**, 17732.

37 Z. Peng and X. Peng, *J. Am. Chem. Soc.*, 2001, **123**, 183.

38 B. A. Sperling and W. J. Parak, *Philos. Trans. R. Soc., A*, 2010, **368**, 1333.

39 W. R. Algar and U. J. Krull, *ChemPhysChem*, 2007, **8**, 561.

40 M. T. Frederick, V. A. Amin and E. A. Weiss, *J. Phys. Chem. Lett.*, 2013, **4**, 634.

41 Y. J. Zhang, A. M. Schnoes and A. R. Clapp, *ACS Appl. Mater. Interfaces*, 2010, **2**, 3384.

42 S. F. Wuister, C. D. M. Donegá and A. Meijerink, *J. Phys. Chem. B*, 2004, **108**, 17393.

4634 | *J. Mater. Chem. C*, 2017, **5**, 4629–4635

This journal is © The Royal Society of Chemistry 2017

43 A. M. Smith, H. Duan, M. N. Rhyner, G. Ruan and S. Nie, *Phys. Chem. Chem. Phys.*, 2006, **8**, 3895.

44 H. Li, W. Shi, W. Shi, L. Chen, S.-J. Tsengand and S. Tangb, *Nanotechnology*, 2008, **19**, 475101.

45 G. H. T. Au, W. Y. Shih and W. H. Shih, *Mater. Res. Express*, 2015, **2**, 015401.

46 T. Nann, *Chem. Commun.*, 2005, 1735.

47 I. Mekis, D. V. Talapin, A. Kornowski, M. Haase and H. Weller, *J. Phys. Chem. B*, 2003, **107**, 7454.

48 X. Zhong, M. Han, Z. Dong, T. J. White and W. Knoll, *J. Am. Chem. Soc.*, 2003, **125**, 8589.

49 D. V. Talapin, I. Mekis, S. Gotzinger, A. Kornowski, O. Benson and H. Weller, *J. Phys. Chem. B*, 2004, **108**, 18826.

50 M. V. Yezhelyev, L. Qi, R. M. O'Regan, S. Nie and X. Gao, *J. Am. Chem. Soc.*, 2008, **130**, 9006.

51 Q. S. Feng, L. J. Dong, J. Huang, Q. Li, Y. H. Fan, J. Xiong and C. X. Xiong, *Angew. Chem., Int. Ed.*, 2010, **49**, 9943.

52 W. Yu, A. Wang and X. Peng, *Chem. Mater.*, 2003, **123**, 1389.

53 J. N. Demas and G. A. Crosby, *J. Phys. Chem.*, 1971, **208**, 205.

54 C. Carrillo-Carrion and W. J. Parak, *J. Colloid Interface Sci.*, 2016, **478**, 88.

55 R. K. Ratnesh and M. S. Mehata, *Spectrochim. Acta, Part A*, 2017, **179**, 201.

56 H. Zheng, L. J. Mortensen and L. A. DeLouise, *J. Biomed. Nanotechnol.*, 2013, **9**, 3.

57 W. Guo, J. J. Li, Y. A. Wang and X. Peng, *Chem. Mater.*, 2003, **15**, 3125.

58 L. Huang, M. Liao, S. Chen, V. G. Demillo, S. A. Dupre, X. Zhu, N. G. Publicover and K. W. Hunter, *J. Nanopart. Res.*, 2014, **16**, 8.

59 Y. Wang, Z. Tang, M. A. Correa-Duarte, I. Pastoriza-Santos, M. Giersig, N. A. Kotov and L. M. Liz-Marzan, *J. Phys. Chem. B*, 2004, **108**, 15461.